



Zhang, W., Zhou, J., Huang, Y., Akinsolu, M. O., He, M. and Liu, B. (2021) A Dual-Band Metasurface-Based Antenna with Shorting Pins. In: 2021 IEEE MTT-S International Microwave Workshop Series on Advanced Materials and Processes for RF and THz Applications (IMWS-AMP), Chongqing, China, 15-17 Nov 2021, pp. 240-242. ISBN 9781665428194

(doi: [10.1109/IMWS-AMP53428.2021.9643878](https://doi.org/10.1109/IMWS-AMP53428.2021.9643878))

This is the Author Accepted Manuscript.

© 2021 IEEE. Personal use of this material is permitted. Permission from IEEE must be obtained for all other uses, in any current or future media, including reprinting/republishing this material for advertising or promotional purposes, creating new collective works, for resale or redistribution to servers or lists, or reuse of any copyrighted component of this work in other works.

There may be differences between this version and the published version. You are advised to consult the publisher's version if you wish to cite from it.

<http://eprints.gla.ac.uk/253464/>

Deposited on: 1 October 2021

A Dual-Band Metasurface-Based Antenna with Shorting Pins

Wenzhang Zhang, Jiafeng Zhou, Yi Huang
Department of Electrical Engineering and
Electronics
University of Liverpool
Liverpool

W.Zhang29@liverpool.ac.uk; jiafeng.zhou@li
verpool.ac.uk; yi.huang@liverpool.ac.uk.

Mobayode O. Akinsolu
Faculty of Arts, Science and Technology
Wrexham Glyndwr University
Wrexham
m.o.akersolu@ieee.org

Mingwei He, Bo Liu
James Watt School of Engineering
University of Glasgow
Glasgow
2357804H@student.gla.ac.uk;
liubo168@gmail.com

Abstract—A dual-band metasurface (MTS)-based antenna can be realized by composite right-/left-handed (CRLH) structures for wireless power transfer or ambient wireless energy harvesting. The bandwidth in the right-handed (RH) region can be obtained by exciting different desired transverse magnetic (TM) modes while that in the left-handed (LH) region can be achieved by mushroom radiating structures. The position choice of shorting pins in mushroom structures is significant since it will not only affect the potential bandwidth in the RH region, but also be related to the resonant frequencies in the LH region. The positions of the shorting pins will be chosen where the Electric field distribution is minimal for modes excited in the RH region. The proposed dual-band MTS-based antenna with an overall size of $0.375 \lambda_0 \times 0.375 \lambda_0 \times 0.035 \lambda_0$ can achieve 25% and 48% fractional bandwidths, and 5.0 and 9.6 dBi peak gains in the lower and higher frequency band, respectively.

Keywords—Broadband, Dual-band, Metasurface.

I. INTRODUCTION

Due to the rapid growth of wireless communication systems, dual or multiple broadband antennas are in increasing demand [1]-[2]. A conventional patch antenna suffers from the inherent limitation of narrow bandwidth. Recently, metasurface (MTS)-based antennas have been proposed to increase the bandwidth of antennas. The bandwidth can be enhanced by placing an MTS right below or above a feeding aperture. Among these MTS-based antennas, only a limited number of them can achieve dual-band performance [3]-[7].

To realize a dual-band antenna based on MTS, one effective method is to use a composite right-/left-handed (CRLH) structure, where mixed contributions of both the left-handed (LH) and right-handed (RH) structures are utilised. A CRLH mushroom unit cell contains an equivalent series capacitance and an equivalent shunt inductor mainly contributed by the LH structures at the lower frequency band, and a series inductor and a shunt capacitance mainly contributed by the RH structure at the higher frequency band. The gaps between the metallic radiating elements can provide series capacitance and the shoring pins connected between radiating elements and the ground plane can be viewed as shunt inductors. The metallic radiating elements can be considered as series inductor and the gaps between radiating elements and the ground plane can be seen as shunt capacitors [8].

However, there exist limitations of using CRLH structures to design dual broadband MTS-based antennas. At the higher frequency band, different TM modes operating in the RH region are normally excited to achieve a broad bandwidth [5]-[7]. By introducing shorting pins between metallic radiating elements and the ground plane, a radiation band at lower frequency band can be realized. But the shorting pins may also affect (suppress) the modes in the RH region as well since they can shorten the electrical lengths of the modal currents. If the shorting pins are positioned at the maximum E-field places of the excited modes in the RH region, the bandwidth will be affected. Thus, determining the positions of shorting pins becomes a significant task if both bandwidths at the lower and higher frequency bands are to be kept.

This paper proposes a dual broadband MTS-based antenna for several wireless applications covering LTE, WiFi, WiMax, and 5G sub 6 GHz bands, which can be used as the receiver in the wireless power transfer or energy harvesting systems. The proposed antenna consists of seven hexagonal radiating elements with six parasitic elements on the MTS layer, fed by an aperture-coupled structure with a H-shape slot on the ground plane. One broad bandwidth in the RH region is realised by exciting multiple MTS modes. The other broad bandwidth at the lower frequency band is realized in the LH region by adding shorting pins to the radiation elements. To keep the bandwidth performance at the higher frequency band, the positions of the shorting pins should be chosen at the minimum E-field places at each excited mode at the higher frequency band. Since the current distributions and E-field distributions on the MTS layer of specific modes (e.g. TM₀₁ mode) can be analyzed, the positions of the shorting pins can be derived accordingly. The proposed dual-band MTS-based antenna with an overall size of $0.375 \lambda_0 \times 0.375 \lambda_0 \times 0.035 \lambda_0$ can achieve 25% and 48% fractional bandwidths, and 5.0 and 9.6 dBi peak gains in the lower and higher frequency bands, respectively.

II. ANTENNA DESIGN

A. Potential Modes in MTS-based Antennas

An MTS-based antenna with hexagonal radiating elements was designed. In this model, if a feeding structure is aperture-coupled positioned in the middle of the feeding slot, only TM modes will be excited. Apart from the fundamental TM₀₁ mode, the higher TM_{xy} mode can also be excited. For higher TM_{xy}

mode, the value of x is mainly determined by the feeding

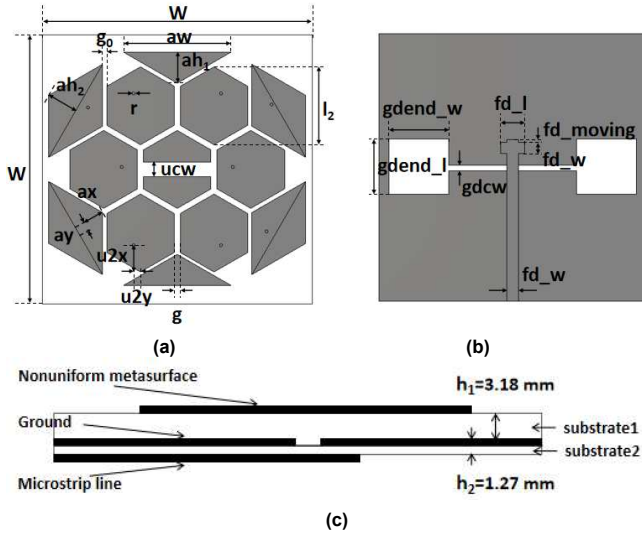


Fig. 1. Geometry of the proposed MTS antenna using nonuniform unit cells. (a) Top view. (b) Bottom view. (c) Side view. ($W=45$ mm, $l_2=13$ mm, $aw=18$ mm, $ah_1=5.2$ mm, $ah_2=5.2$ mm, $g=0.8$ mm, $g_0=0.7$ mm, $ucw=2.3$ mm, $r=0.25$ mm, $u_2x=4.5$ mm, $u_2y=1.2$ mm, $ax=3.7$ mm, $ay=1.5$ mm, $fd_w=1.9$ mm, $fd_l=4$ mm, $fd_moving=0.5$ mm, $gdcw=0.9$ mm, $gdend_w=10$ mm, $gdend_l=9.3$ mm).

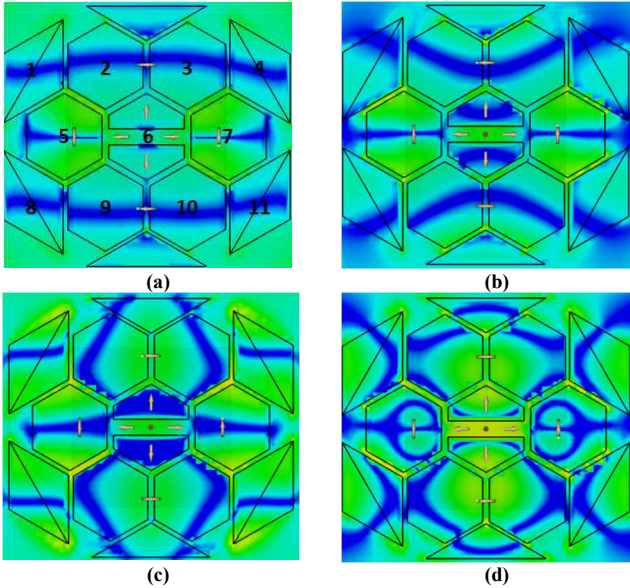


Fig. 2. Electric field distributions of the proposed MTS antenna at four resonant frequencies in the higher frequency band, at (a) 5.0, (b) 5.8, (c) 7.0 and (d) 7.6 GHz.

structure while the value of y is mainly determined by the radiating gaps which are parallel to the aperture on the ground plane.

For the fundamental TM_{01} mode, the minimum E-field places mainly concentrate on the centre of each radiating element. Different from the fundamental mode, the higher TM modes like TM_{12} can be possibly excited at different radiating positions corresponding to different resonant frequencies. The

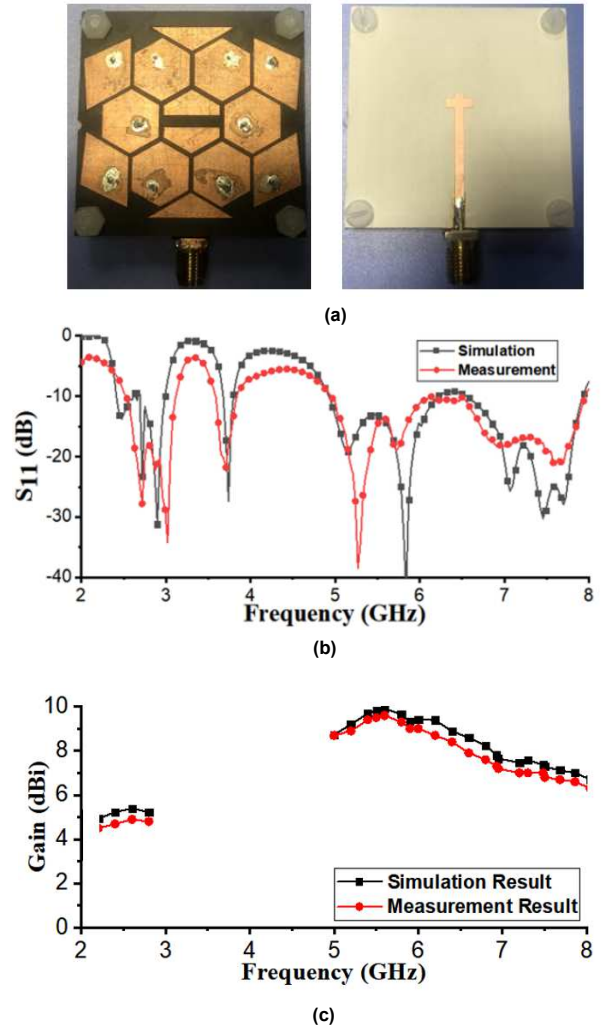


Fig. 3. (a) Photographs of the fabricated antenna. Simulated and measured (b) S-parameters and (c) gains of the proposed antenna.

minimum E-field distributions of the higher TM mode will exist at the corner of the unit cells in the second and fourth row.

B. Proposed Antenna Structure

For the antenna structure shown in Fig. 1, to excite desired modes in the higher frequency band as mentioned in the previous section, firstly, a basic MTS-based antenna using seven hexagonal radiating elements with a centre slot is designed. Next, to further improve the impedance bandwidth six triangular or quadrilateral parasitic elements are added around the hexagonal radiating elements.

Then, to excite modes in the LH region at around 2.45 GHz, shorting pins are added at several radiating elements. The positions of the shorting pins affect the bandwidths both at the lower frequency and the higher frequency band. The positions are chosen according to two considerations. The first consideration is that the pins should have too much effect on the

desired modes excited in the higher frequency band. That means the shorting pins should be added at the nulls of the electric field distribution. As can be seen from Fig. 2, the positions of common nulls of E-field distributions at these four frequencies are around upper-right part of unit 1 and unit 3, lower-right part of unit 8 and unit 10, upper-left part of unit 2 and unit 4, lower-

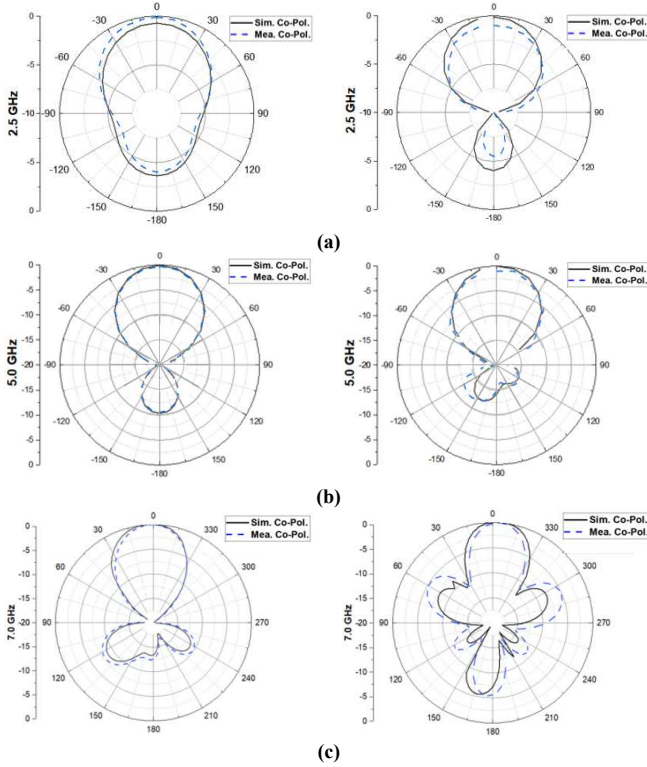


Fig. 4. Simulated and measured radiation patterns of the proposed antenna at (a) 2.5 GHz, (b) 5.0 GHz and (c) 7.0 GHz.

left part of unit 9 and unit 11, and the center part of unit 5 and unit 7. The second consideration is that the positions of the shorting pins will affect the values of series capacitance and shunt inductance that determine the resonant frequencies of the modes in the LH region.

According to these two considerations, the positions of the shorting pins were chosen as shown in Fig. 1(a). The geometry and detailed dimensions of the MTS layer and the feeding layer are shown in Fig. 1(a) and (b). These two layers are coupled through an H-shaped aperture. A Rogers RT5870 substrate was used for the first and second layers, whose dielectric constant and thickness are 2.33 and 3.18 mm, respectively. An alternative substrate material, TMM6 (dielectric constant = 6.0 and thickness = 1.27 mm), was used to support the ground plane and the feed line.

III. SIMULATED AND MEASURED RESULTS

An MTS-based antenna with hexagonal radiating element and parasitic elements was prototyped and measured to validate the proposed design method, as shown in Fig. 3(a). Detailed dimensions of the proposed antenna are provided in Fig. 1.

Fig. 3(b) presents a comparison between the simulated and measured S-parameters. In the lower frequency band, the

simulated -10-dB impedance bandwidth is of 2.25-2.9 GHz or 25% while in the higher frequency band, the simulated -10-dB impedance bandwidth is from 4.95 to 8.35 GHz or 50%. Reasonable agreement is observed between the simulated and the measured results. The difference between simulated and measured results is due to the fabrication precision, especially the tightness between two substrate materials, which will have a greater effect on higher resonant frequencies. The comparison between the simulated and the measured gain of the antenna is also described in Fig. 3(c). The simulated gains over the lower band and the higher band vary within 4.8-5.4 dBi and 6.3-9.8 dBi, which agree well with the measured gains.

The normalized radiation patterns of the proposed antenna in the lower and higher frequency band at 2.5, 5.0 and 7.0 GHz are shown in Fig. 4. Due to the symmetry of the feeding structure, both the simulated and measured cross-polarization levels at boresight are below -30 dB in both the xoz and yoz planes. As can be seen, the proposed antenna has a very directional radiation pattern at 2.5 and 5.0 GHz while the radiation pattern at 7.0 GHz has slightly higher side lobes.

IV. CONCLUSIONS

In this paper, a dual-band MTS-based antenna using the CRLH mushroom structure is proposed. The key design part is to choose the positions of the shorting pins in mushroom radiating elements since it will affect both the lower and higher bandwidth significantly. The proposed antenna has a low profile and compact size, which is suitable for wireless power transfer or energy harvesting systems. The simulated and measured results are in good agreement, which verifies the proposed MTS-based antenna design method.

REFERENCES

- [1] Ying Liu, Sihao Wang, Na Li, Jing-Bo Wang, and Jianping Zhao, "A Compact Dual-Band Dual-Polarized Antenna With Filtering Structures for Sub-6 GHz Base Station Applications," *IEEE Antennas and Wireless Propagation Letters*, vol. 17, no. 10, 2018, pp. 1764-1768.
- [2] Yuehui Cui, Xuanbo Wang, Guoyan Shen, and RongLin Li, "A Triband SIW Cavity-Backed Differentially Fed Dual-Polarized Slot Antenna for WiFi/5G Applications," *IEEE Transactions on Antennas and Propagation*, vol. 68, no. 12, Dec. 2020, pp. 8209-8214.
- [3] Teng Li and Zhi Ning Chen, "Shared-Surface Dual-Band Antenna for 5G Applications," *IEEE Transactions on Antennas and Propagation*, vol. 68, no. 2, 2020, pp. 1128-1131.
- [4] Teng Li and Zhi Ning Chen, "Metasurface-Based Shared-Aperture 5G S-/K-Band Antenna Using Characteristic Mode Analysis," *IEEE Transactions on Antennas and Propagation*, vol. 66, no. 12, Dec. 2018, pp. 6742-6750.
- [5] Teng Li and Zhi Ning Chen, "A Dual-Band Metasurface Antenna Using Characteristic Mode Analysis," *IEEE Transactions on Antennas and Propagation*, vol. 66, no. 10, Oct. 2018, pp. 5620-5624.
- [6] Botao Feng, Xiaoyuan He, Jui-Ching Cheng, and Chow-Yen-Desmond Sim, "Dual-Wideband Dual-Polarized Metasurface Antenna Array for the 5G Millimeter Wave Communications Based on Characteristic Mode Theory," *IEEE Access*, vol. 8, 2020, pp. 21589-21601.
- [7] Zhao Wu, Long Li, Xi Chen, and Ke Li, "Dual-Band Antenna Integrating With Rectangular Mushroom-Like Superstrate for WLAN Applications," *IEEE Antennas and Wireless Propagation Letters*, vol. 15, 2016, pp. 1269-1272.
- [8] Nader Engheta and Richard W. Ziolkowski, *Metamaterials: Physics and Engineering Explorations*, A John Wiley & Sons, Inc.